

FLIGHT TESTS OF HELICOPTER NOISE ABATEMENT OPERATIONS

Hirokazu Ishii, Hiromi Gomi, and Yoshinori Okuno
Japan Aerospace Exploration Agency
Mitaka, Tokyo, Japan

Junichi Uchida and Takeshi Tsuchiya
The University of Tokyo
Bunkyo, Tokyo, Japan

Abstract

The Japan Aerospace Exploration Agency is researching technologies to reduce the noise impact on the ground from helicopters: trajectory optimization and a cockpit display system to show pilots the aircraft's acoustic footprint in real-time. These technologies use a simple noise model which has been developed based on flight test measurements. This paper shows the result of flight tests conducted to validate the noise model and to evaluate the effectiveness of these technologies for helicopter noise abatement operations.

Nomenclature

d	distance between aircraft and observer
d_{ref}	reference distance (100m)
g	acceleration of gravity
h	altitude ($= -Z$)
m	aircraft mass
t	time
w	weighting coefficient
J	cost function
L_A	noise level at an observer
L_m	average noise level
L_{AE}	sound exposure level
L_{src}	noise level at reference distance
ΔL_{inv}	spherical spreading loss
ΔL_{air}	atmospheric absorption
ΔL_{EGA}	excess ground attenuation
N	number of microphones
T	thrust
T_0	reference time (1sec)
V	horizontal speed
W	descent rate
X, Y, Z	aircraft position
Φ	roll angle
Θ	pitch angle
Ψ	yaw angle
(\cdot)	time differential

Introduction

The Japan Aerospace Exploration Agency (JAXA) is carrying out a research program named NOCTARN (New Operational Concept using Three-dimensional Adaptable Route Navigation), aimed at developing an aircraft operational concept to enhance the capacity and efficiency of small regional airports (Ref. 1). One goal of this research is to reduce the noise impact to communities around such airports by using curved approach paths with consideration to the cumulative noise emitted by other aircraft.

In order to design noise countermeasures, a noise model is necessary to predict noise impact on the ground. Helicopter noise contains sounds from various sources such as rotors, engines, and gearbox, and their frequency and directivity characteristics vary according to the flight condition. Although recent advances in computer and calculation technology have improved the effectiveness of CFD (computational fluid dynamics) to analyze aerodynamically-induced noise and noise propagation characteristics, and much research has been carried out to reveal the mechanisms of noise generation, especially main rotor noise (e.g. Ref. 2), a combination of analytical and empirical methods is the best means to predict overall helicopter noise in actual flight in real-time.

JAXA has been conducting various acoustic flight tests using its research helicopter (Fig. 1, Ref. 3), a twin turboshaft 4500kg machine with a four-bladed main rotor, to obtain basic noise data during straight (level, descending, and climbing) flight and turning flight conditions (Ref 4, 5). The noise model introduced here was developed based on the data obtained from these flight tests. Since the model is intended to be used for real-time prediction, it is simplified to reduce the computational load. The noise model is used in two technologies for noise reduction: optimization of approach flight paths and a cockpit display to inform pilots of noise impact predicted onboard in real-time. This paper also presents an overview of these technologies and the results of flight tests conducted to examine their feasibility and effectiveness.

Noise Model Based on Flight Test Results

In order to develop a simplified noise model that can be used for real-time noise prediction, noise measurements obtained from flight tests were reduced to an omnidirectional source model and theoretical and empirical attenuation models were used to calculate the noise levels on the ground.

Source Model

Helicopters radiate an excessive slap noise called blade-vortex interaction (BVI) noise during approach, and this is known as one of the most annoying sources of noise emitted by helicopters during terminal operations. BVI noise is generated by impulsive pressure fluctuations on main rotor blades induced by tip vortices shed by the preceding blades. Since the tip vortices pass in close proximity of the blades at “moderate” descent angles, strong BVI noise is radiated during conventional approach flight paths.

Since BVI noise often becomes dominant in terminal operations as described above, the source model should predict the trend of BVI noise. JAXA has conducted flight tests to determine the relationship between BVI noise level and flight condition utilizing an onboard external microphone installed at the tip of a nose boom as shown in Fig. 2. Since measurement using an onboard microphone can be conducted at

high altitude, flight is not constrained by proximity to the ground and noise data can be obtained over a wide range of vertical speeds. Various combinations of airspeed and vertical speed were flown and noise levels (A-weighted overall sound pressure levels) were derived from the sound measurements as shown in Fig. 3. It can be seen that the noise level strongly depends on flight path angle, shown as black lines. The red markers in Fig. 4 show the noise level replotted as a function of flight path angle. The maximum noise levels are due to BVI noise and are observed at flight path angles of around -5 degrees. The relationship between noise level and flight path angle is modeled as the dashed line.

Whereas a nose microphone is appropriate for obtaining the relationship between BVI noise level and flight condition, ground microphones are needed to measure the noise footprint on the ground, which is affected by noise propagation characteristics. JAXA therefore also conducted flight tests using ground microphones to measure noise directly below the helicopter’s flight path. The blue markers in Fig. 4 show the maximum noise levels obtained during level flight at an airspeed of 100kt and an altitude of 300ft



Fig. 1. JAXA’s research helicopter.

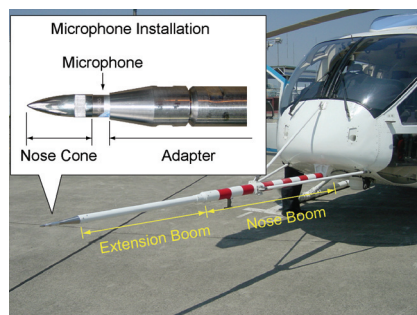


Fig. 2. An overview of the nose microphone.

(91m). Here, the noise levels are calculated for a point 100m from the aircraft by compensating attenuation due to omnidirectional radiation (spherical spreading from a point source) and atmospheric absorption. Then, the relationship between noise level and flight path angle shown as the dashed line is compensated so that the noise model shown as the solid line agrees with the noise levels measured by the ground microphone.

A helicopter's noise emission also varies according to bank angle in turning flight. Figure 5 shows the relationship between measured noise level and bank angle at an airspeed of 100kt and an altitude of 260ft (79m). The blue markers indicate noise levels at a distance of 100m estimated from the measured data by the same method as above.

In the noise model derived from these flight tests, the noise level at a reference distance (100m) L_{src} [dBA] is written as a function of a flight path angle γ [deg], and a bank angle Φ [deg].

$$L_{src} = \begin{cases} 80 + 0.1(\gamma + 15) - 80 \log_{10}[\cos(\Phi\pi/180)] \\ \quad (\gamma < -15 \text{ or } \gamma > 5) \\ 80 + 0.1(\gamma + 15) + 3[1 + \cos(0.1(\gamma + 5)\pi)] \\ \quad - 80 \log_{10}[\cos(\Phi\pi/180)] \\ \quad (-15 \leq \gamma \leq 5) \end{cases}$$

Helicopter noise, especially BVI noise, has a strong directionality. Although the authors have examined the noise directivity patterns of JAXA's research helicopter from ground measurements as shown in Fig. 6 (Ref. 4), insufficient data were obtained to model the directivity in all directions. Hence, the noise source model is represented as an omnidirectional point source, which also reduces the computational load.

Propagation Model

Sound is attenuated during propagation, and there are analytical models to estimate attenuation due to omnidirectional radiation (spherical spreading) and atmospheric absorption. In general, there is a discrepancy between the sum of these models and the actual attenuation due to a residual effect called excess ground attenuation, which consists of ground attenuation and the influence of weather conditions.

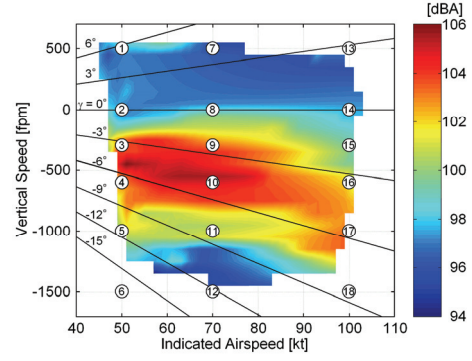


Fig. 3. The relationship between noise level and flight path angle measured in flight tests.

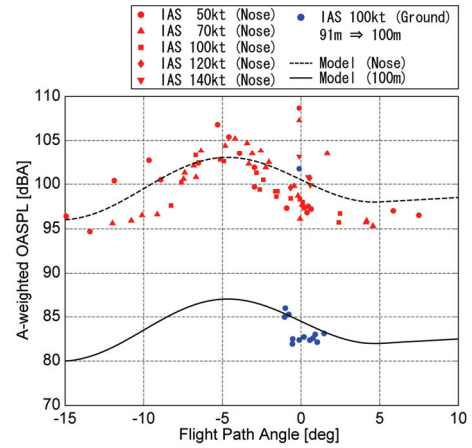


Fig. 4. The source model in straight flight based on flight test results.

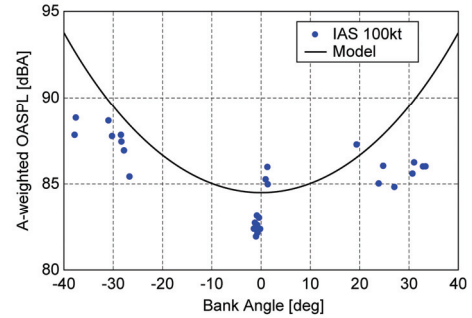


Fig. 5. Effect of turning flight on noise level based on flight test results.

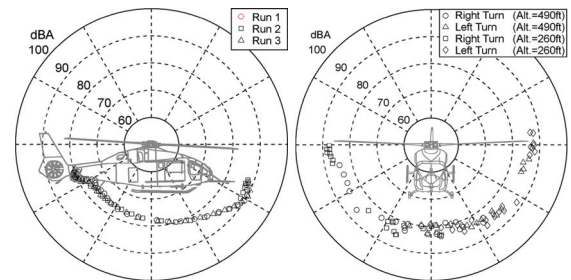


Fig. 6. Directivity patterns estimated from the results of measurement on the ground.

Spherical spreading loss is derived from the fact that the intensity of sound from a point source diminishes at a rate that is inversely proportional to the square of the propagation distance. Hence the spherical spreading loss, ΔL_{inv} [dB], at a distance, d [m], can be written as

$$\Delta L_{inv} = 20 \log_{10}(d / d_{ref})$$

where d_{ref} is the reference distance (100m).

The atmospheric absorption model in ISO 9613 (Ref. 6) is described in terms of an attenuation coefficient as a function of the following four variables: the frequency of the sound, and the temperature, humidity and pressure of the air. The atmospheric attenuation model in this paper was developed to reflect the noise spectrum characteristics of the research helicopter and atmospheric absorption. The black line in Fig. 7 shows the one-third octave band levels measured during level flight at an airspeed of 100kt and an altitude of 280ft (85m). The red, blue, and green lines show A-weighted one-third octave band levels at distances of 85m, 1000m, and 2000m from the aircraft, respectively. Figure 8 shows the resultant atmospheric absorption, ΔL_{air} , in A-weighted noise level as a function of distance from the aircraft.

Although SAE/AIR 1751 (Ref. 7) is a representative model of excess ground attenuation, it does not include the effect of wind, and so a modified model proposed in Ref. 8 was used in this paper to take account of wind. Figure 9 shows a schematic image of a flight test conducted to verify the model. The measured excess ground attenuation shown in Figure 10 was calculated from the one-third octave band sound pressure level at a midband frequency of 250Hz and compared with the model estimate value. It can be seen that the estimated and measured values have the same trend, and the differences in magnitude are thought to be the effects of ground reflection, which increases the measured noise level at each frequency in the one-third octave band. Since the effect of reflection is included in the measured excess ground attenuation, some measured values of the excess ground attenuation indicate negative values.

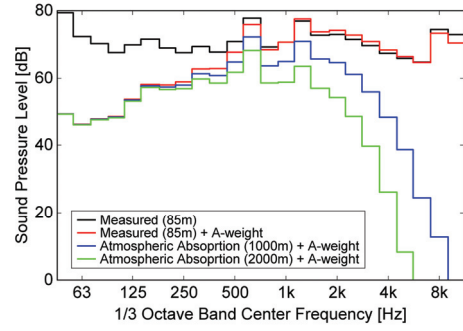


Fig. 7. Effect of atmospheric attenuation at various distance.

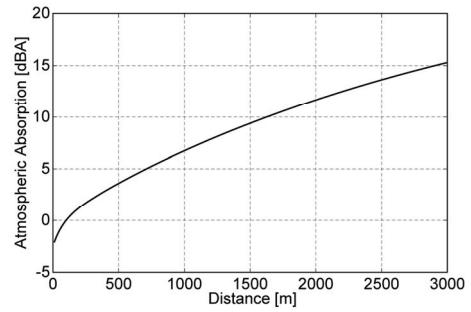


Fig. 8. The atmospheric absorption model. (Temperature=25°C, Humidity=70%, and Pressure=1013.25hPa)

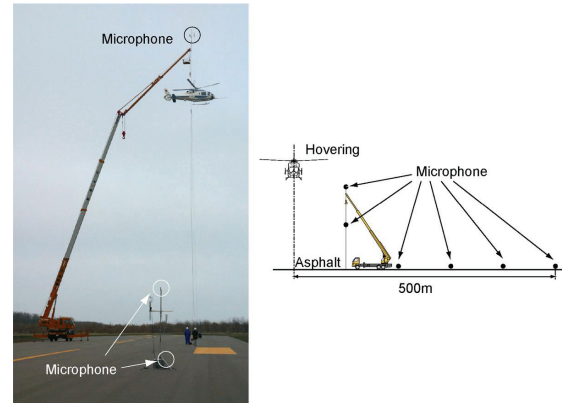


Fig. 9. Schematic image of flight tests to measure the excess ground attenuation.

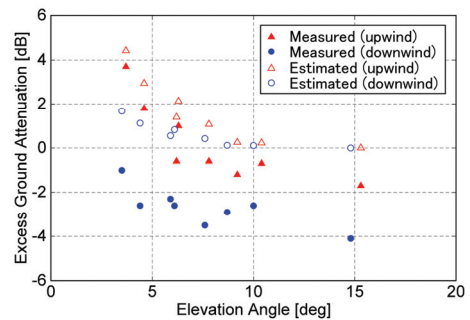


Fig. 10. A comparison of the measured and estimated excessive ground attenuation. (one-third octave band level at a midband frequency of 250Hz)

Trajectory Optimization

JAXA and the University of Tokyo have been jointly researching a method for optimizing helicopter noise abatement approaches. The research objectives are: 1) to find method suitable for optimizing helicopter noise abatement approach paths to reduce cumulative noise impact; 2) to examine appropriate formulations to obtain feasible approach trajectories which can be followed by pilot manual control; and 3) to establish a method to verify the effect of the optimization. In order to afford a good insight into the problem, simplified models are used at this stage.

Aircraft Dynamics Model

The aircraft is represented by a point mass, and only the thrust of the main rotor and the gravitational force act on the aircraft as external forces. The aircraft is controlled by changing the magnitude of the thrust T , the lateral direction of the thrust Φ , and the longitudinal direction of the thrust Θ . Then the equations of motion can be written as

$$\begin{aligned}\dot{X} &= V \cos \Psi \\ \dot{Y} &= V \sin \Psi \\ \dot{Z} &= W \\ \dot{V} &= -\frac{T}{m} \cos \Phi \sin \Theta \\ \dot{W} &= g - \frac{T}{m} \cos \Phi \cos \Theta \\ \dot{\Psi} &= \frac{T}{mV} \sin \Theta\end{aligned}$$

where X , Y , Z are expressed in an NED (North-East-Down) coordinate system with the origin at the landing point, and positive X , Y , and Z axis pointing north, east, and downward, respectively. V and W are horizontal and vertical flight speeds.

Cost Function

Since this research is aimed at minimizing cumulative noise impact over areas around a flight path, the cost function has been determined as a spatially averaged and temporally integrated noise index. Let $L_A(t, i)$ be the noise level at i -th location of an observer on the ground at time t estimated by the noise model described above.

$$L_A(i, t) = L_{\text{src}} - \Delta L_{\text{inv}} - \Delta L_{\text{air}} - \Delta L_{\text{EGA}} \\ (i = 1, 2, \dots, N)$$

The averaged noise level $L_m(t)$ at time t can be obtained by energetically averaging $L_A(i, t)$ over all observer locations.

$$L_m(t) = 10 \log_{10} \left(\frac{1}{N} \sum_{i=1}^N 10^{L_A(t, i)/10} \right)$$

Then, $L_m(t)$ is energetically integrated in the time domain to obtain a noise index to be minimized.

$$L_{\text{AE}} = 10 \log_{10} \frac{1}{T_0} \int_0^{t_f} 10^{L_m(t)/10} dt$$

where reference time T_0 is defined as 1 second so that L_{AE} represents the sound exposure level from the averaged noise level.

In order to avoid obtaining an optimum solution with oscillatory control variables, the sum of the square of the control variables are added to noise index L_{AE} , and the cost function J is written as

$$J = L_{\text{AE}} + w \int_0^{t_f} \left\{ (T-1)^2 + \Theta^2 + \Phi^2 \right\} dt$$

where a weighting coefficient w is defined as an appropriate value such that the control variables do not become oscillatory.

Constraints

Since the generated optimized noise abatement flight trajectories are to be followed by manual control, constraints must be defined appropriately to obtain trajectories which can be flown safely without excessive pilot workload. Preliminary flight simulator tests were conducted prior to actual flights to examine appropriate constraints, defined as follows

$$\begin{aligned}\text{Airspeed:} \quad & 50 \leq V \leq 100 \quad [\text{kt}] \\ \text{Descent rate:} \quad & 0 \leq W \leq 800 \quad [\text{fpm}] \quad (h \geq 480\text{ft}) \\ & 0 \leq W \leq \frac{5}{3}h \quad [\text{fpm}] \quad (h < 480\text{ft}) \\ \text{Acceleration:} \quad & |\dot{V}| \leq 1.5 \quad [\text{kt/sec}] \\ & |\dot{W}| \leq 100 \quad [\text{fpm/sec}] \\ \text{Roll angle:} \quad & |\Phi| \leq 15 \quad [\text{deg}]\end{aligned}$$

Initial/Terminal Conditions

Five observer positions were located around an airspace as shown in Fig. 11 and Table 1. Since the helicopter was flown manually, the terminal point of the approach trajectories was defined to be 300ft above the ground with consideration to safe landing. Then, the terminal point (X,Y) was defined along the runway direction so that the descent angle between the terminal position and the touch down point was 6 degrees, which is normally flown by helicopters in approach flight. Thus, the initial and terminal conditions were defined as follows

$$\text{Initial conditions: } \begin{pmatrix} X \\ Y \\ h \\ V \\ W \\ \Psi \end{pmatrix} = \begin{pmatrix} -2.987 & [\text{NM}] \\ -2.186 & [\text{NM}] \\ \text{free} & [\text{ft}] \\ 100 & [\text{kt}] \\ 0 & [\text{fpm}] \\ 26.4 & [\text{deg}] \end{pmatrix}$$

$$\text{Terminal Conditions: } \begin{pmatrix} X \\ Y \\ h \\ V \\ W \\ \Psi \end{pmatrix} = \begin{pmatrix} -0.136 & [\text{NM}] \\ -0.450 & [\text{NM}] \\ 300 & [\text{ft}] \\ 50 & [\text{kt}] \\ \text{free} & [\text{fpm}] \\ 73.2 & [\text{deg}] \end{pmatrix}$$

where h represents altitude ($h = -Z$).

Numerical Solutions

The optimization problem formulated above was solved using the DCNLP (Direct Collocation with Nonlinear Programming) method, which is a common method to solve optimal control problems (Ref. 9). The method employs cubic polynomials to represent state variables, linearly interpolates control variables, and uses collocation points to satisfy the differential equations. As a result, the optimal control problem can be transformed to a mathematical programming problem, and thus it is solved by a sequential quadratic program.

Flight Tests

Flight tests were conducted using JAXA's research helicopter in order to evaluate the effect of the approach path optimization and to examine the validity of the formulations of the optimization program. A "Tunnel-in-the-Sky" display (Ref. 10) shown in Fig. 12 was utilized to guide the pilot along the optimized trajectory.

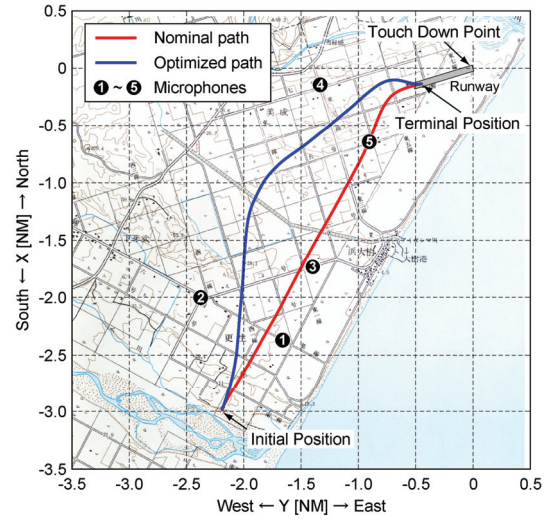


Fig. 11. A comparison between the nominal and optimized paths.

Table 1. The microphone positions

MIC No.	X [NM]	Y [NM]	Z [m]
1	-2.37	-1.66	3.00
2	-2.00	-2.38	-5.60
3	-1.74	-1.40	5.10
4	-0.146	-1.33	-2.10
5	-0.644	-0.905	1.30

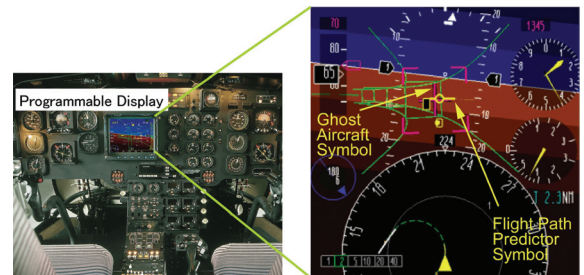


Fig. 12. An example of "Tunnel-in-the-Sky" display image.

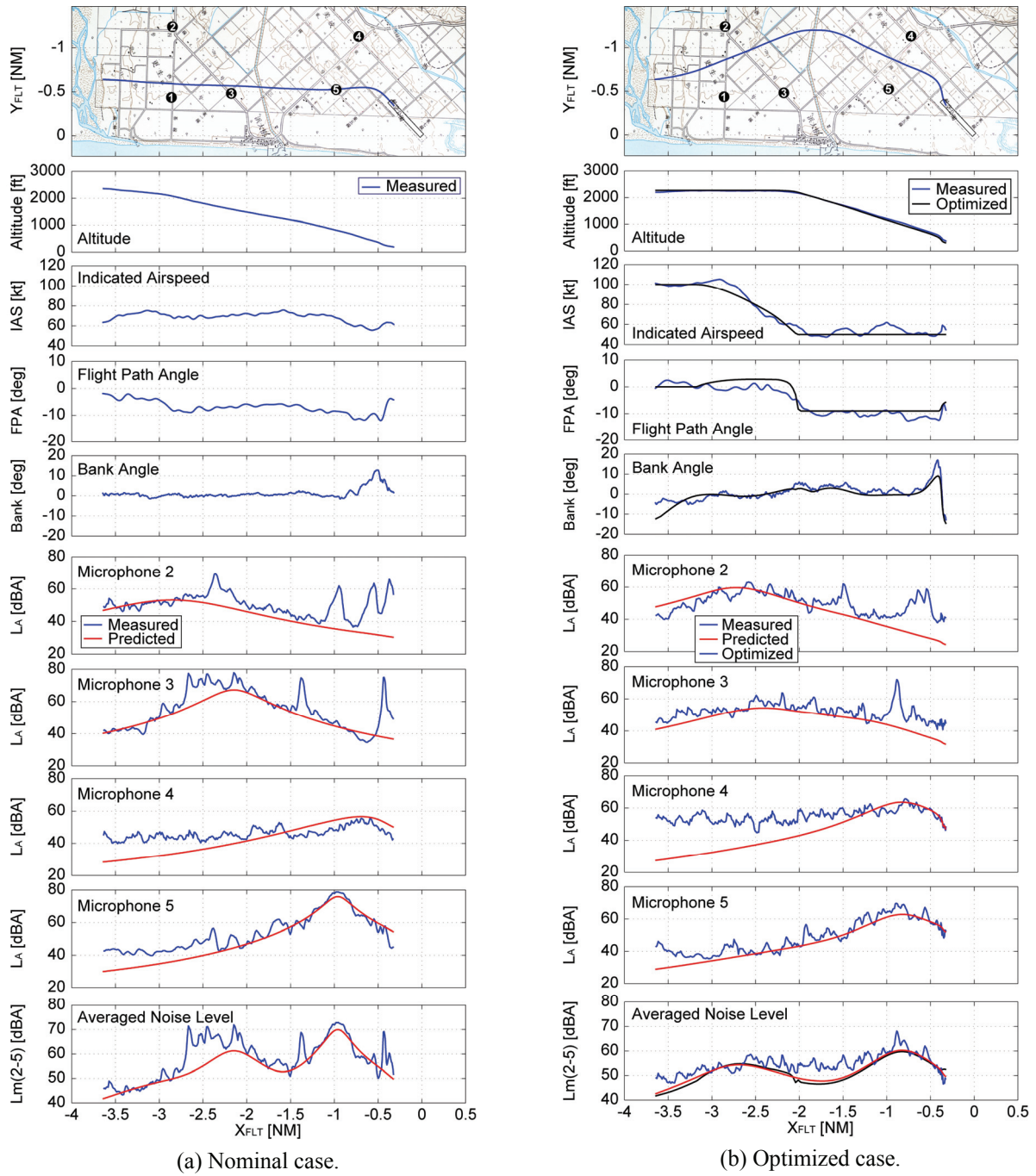


Fig. 13. A comparison of flight conditions and noise levels between the nominal and the optimized case.

Table 2. Validation of the noise prediction accuracy and the effect of optimization.

	Nominal	Optimized	Effect of Optimization
Optimum	N/A	77.6	N/A
Measured	86.2	79.6	6.6
Predicted from Flight data	82.3	76.9	5.4

Unit: [dBA]

Figure 13 shows the flight conditions and noise levels at the observer locations measured by ground microphones. (However, the measurements at observer location 1 failed to be recorded.) To examine the effect of the optimization, the nominal case shown in Fig. 13a was first flown along a nominal path in an ordinary manner. The flight path consisted of straight level and descending segments. The blue and red lines indicate the measured noise levels and noise levels predicted by the presented model, respectively. It is shown that the simple noise model can predict the noise levels well. Small fluctuations seen in measured noise levels are thought to be due to background noises such as wind, grass, birds, and so on. Since some microphones were located by roadsides, noise emitted by passing traffic was also picked up, e.g. peaks of noise level shown at $X_{FLT}=-1\text{NM}$ and -0.5NM at location 2.

The optimized path was then flown, the results of which are shown in Figure 13b. Since the noise source model has a peak value at a descent angle of about 5 degrees, the optimized path has a steeper descent angle. Although the pilot had to control the aircraft in different manner from ordinary flight, he was able to track the optimized path accurately. Table 2 shows a comparison of noise indices L_{AE} between the nominal and optimized cases. Although there are differences between the measured and the predicted levels, the effect of the optimization, that is, the difference between the nominal and the optimized cases, are well predicted by the noise model.

Real-Time Noise Contour Display

Helicopters are usually flown under VFR (Visual Flight Rules) and pilots normally select the flight path and flight conditions considering the noise impact on the ground. However, lack of knowledge of the land use, especially when pilots are flying in unfamiliar areas, can cause excessive noise to be radiated to noise sensitive areas. Moreover, since the directionality of helicopter noise causes a difference between the cabin noise heard by pilots and the noise observed on the ground, in practice helicopters can severely affect noise sensitive areas even though pilots try to reduce the noise impact.

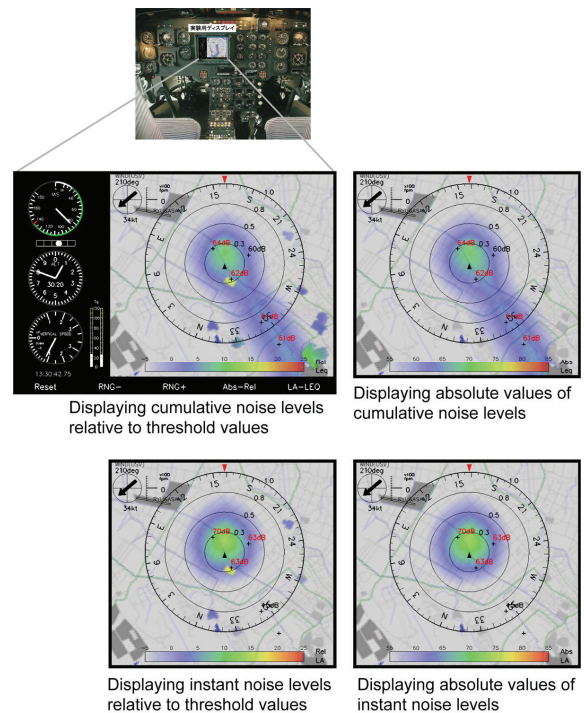


Fig. 14. Examples of RTNC display images corresponding to noise indices to be displayed.

The authors have developed a prototype cockpit display system named the “Real-Time Noise Contour (RTNC)” display, which shows the predicted noise levels on the ground as a contour image superimposed on a map (Fig. 14). This system is aimed to reduce noise impact caused by: 1) the cumulative noise emitted by a single helicopter flying for a prolonged period over a certain area, e.g. sightseeing and newsgathering flights; 2) the cumulative emitted by many helicopters flying a specific path, such as an approach path.

Method of RTNC Image Generation

Figure 15 shows the flow to generate the RTNC display image. A noise source model, a map image of the airspace around the airport, and a land use database are installed into the system. The land use database is stored as indices representing schools, residential areas, bodies of water, woodland, factories, airports, and so on, and the corresponding noise threshold values are also stored at grid points. The predicted noise levels at each grid point is shown as a contour plot, which is superimposed on the map with appropriate transparency.

The pilot can select arbitrary the displayed noise

index to be a combination of either instantaneous or cumulative values, and either absolute values or values relative to noise threshold values defined according to the land use. For example, displaying relative cumulative noise level may be effective when a helicopter is flying over a specific area for news gathering, because the pilot can understand how the cumulative noise impact in the area around the point of interest.

The noise threshold for each land use index is defined by two values. The lower threshold represents the minimum noise level at which an observer at a point can hear the helicopter noise, and the upper threshold represents the noise level limit which should not be exceeded for that land use type. That is, if the predicted noise level at a grid point is below the lower threshold value, the point becomes colorless. The color is changed continuously through blue, green, yellow, and orange while the predicted noise level increases between the threshold values. Finally, if the predicted noise level exceeds the upper threshold value, the point is drawn in red.

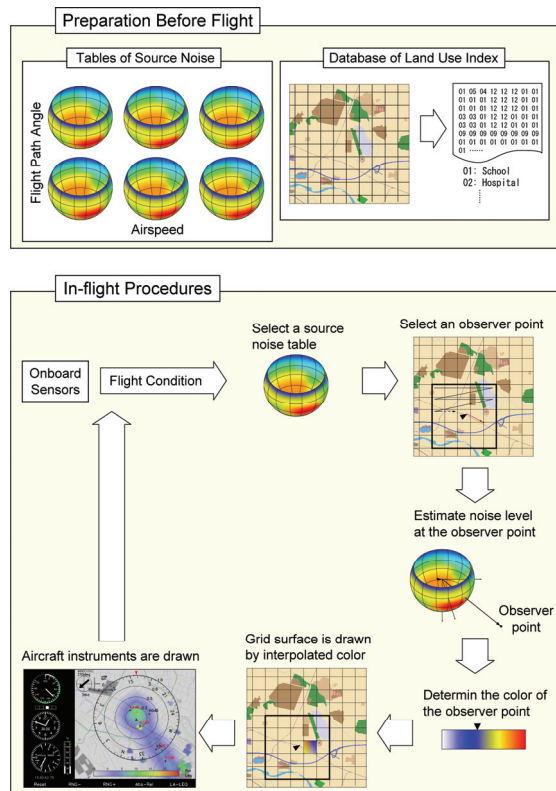


Fig. 15. Outline of RTNC image generation.

In addition to the contour image, the RTNC display can indicate the noise levels at designated points numerically. Figures are normally shown in black, and become red if the noise level exceeds the upper threshold. Since a pilot see the noise levels at these points quantitatively, this function will be useful when the noise impact on the ground is regulated according to measured values.

Flight Tests

Two flight tests were conducted to evaluate the effectiveness of this system in enabling a pilot to reduce the noise impact to a noise sensitive facility, such as a school, near a flight path.

Circling Flight The degree of annoyance caused by noise is dependent on the duration of noise exposure as well as its strength. Therefore, if a helicopter flies over a certain area for a prolonged period, the noise impact in that area will be severe.

The JAXA research helicopter was flown to continuously circle a point to simulate newsgathering photography over an accident site. A nearby virtual noise sensitive facility (such as a school) was prepared at observer location 3 by changing the indices in the land use database.

Figure 16 shows the flight path and noise level at observer location 3, the virtual noise sensitive facility, measured by a ground microphone. The peak values of predicted noise level shows reasonable agreement with the measured peak noise level. Since the noise model does not consider background noise, the predicted noise is smaller than the measured noise when the helicopter is flying away from the microphone. Cumulative noise level was selected and displayed during the flight. The displayed cumulative noise at observer location 3 increased rapidly at around $t = 150\text{sec}$, during the first orbit. Since the RTNC display showed that the noise level at observer location 3 was increasing (Fig. 17), the pilot tried to avoid that location to reduce the noise impact. As a result, the peak values of instantaneous noise level after the second orbit decreased, even though helicopter flew lower on each orbit.

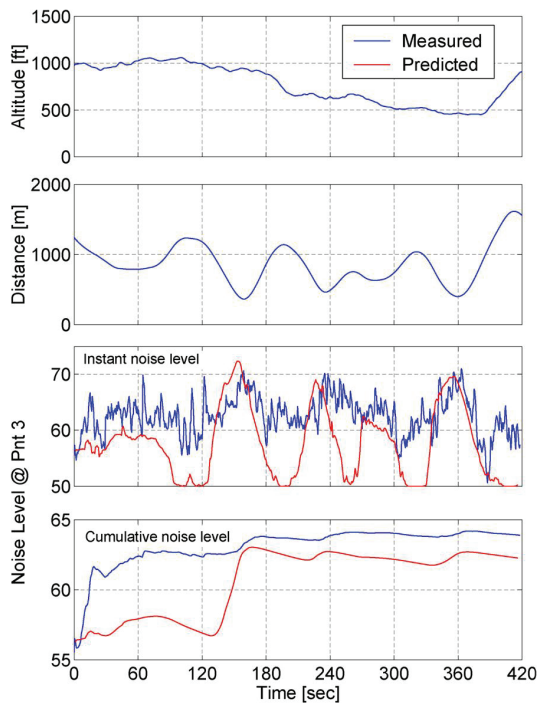
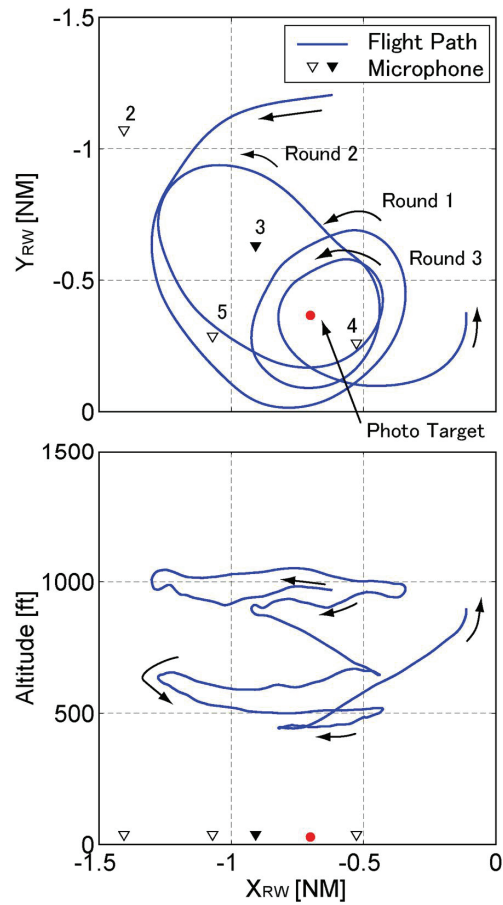


Fig. 16. The effect of the RTNC display in noise reduction during a circular flight.

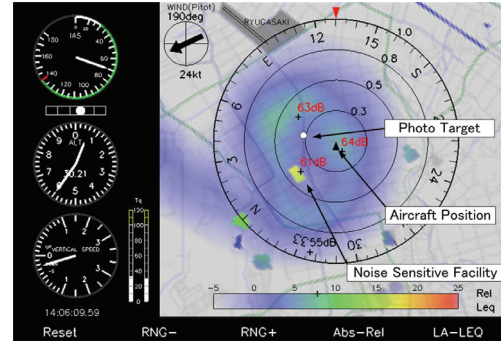


Fig. 17. Example of RTNC display image during a circular flight.

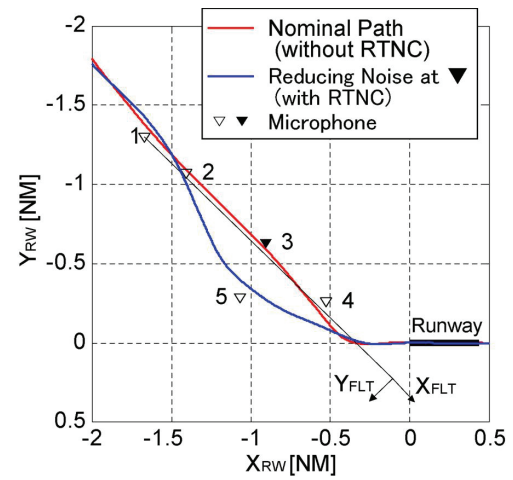


Fig. 18. A comparison of approach paths flown with and without RTNC display.

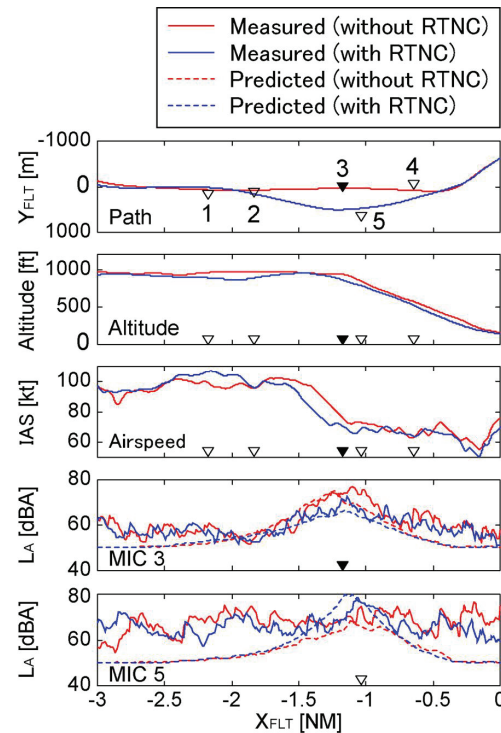


Fig. 19. Variations of flight conditions and noise levels derived by the use of RTNC display during approach.

Approach Flight This test was conducted to evaluate the effectiveness of the RTNC display in reducing the community noise impact of flights along an approach path. It was assumed that there was a noise sensitive area directly under the approach path, which is possible in densely populated areas.

Figure 18 shows flight paths starting at 4NM from a runway, and Fig. 19 shows the flight conditions and noise levels. A virtual noise sensitive facility was prepared at observer location 3 similarly to the circling flight test described above. A nominal case was first flown without the RTNC display, and the flight path indicated by the red line passed over observer location 3. Then, the pilot flew with reference to the RTNC display, and as a result was able to avoid excessive noise impact to observer location 3, as shown by the blue line. This test therefore demonstrated that the pilot was able to successfully avoid flying over the noise sensitive facility with the RTNC display.

Concluding Remarks

Flight tests using JAXA's research helicopter, a twin turboshaft 4500kg machine with a four-bladed main rotor, have been conducted to evaluate two technologies to reduce noise impact, trajectory optimization and the Real-Time Noise Contour (RTNC) display system that shows ground noise levels in real-time.

A simple helicopter noise model has been developed based on flight test noise measurements, and validation tests confirmed that the model predictions show good agreement with measured noise levels.

The results of flight evaluations of trajectory optimization show that: 1) the formulations of the optimization described in this paper are appropriate to obtain flight paths that can be flown manually without excessive workload, 2) noise levels predicted by the simple noise model show reasonable agreement with measured noise levels, and 3) the effect of noise abatement has been demonstrated.

Flight evaluations of the RTNC display system assuming circling flight and an approach over a simulated noise sensitive facility have been conducted, and the results show that flying with reference to the

RTNC display system can reduce the noise impact to noise sensitive areas.

The authors plan to implement the RTNC display system in air traffic control (ATC) workstations developed under NOCTARN research project, which will assist ground controllers to control air traffic with consideration to the noise impact on the ground. In order to develop a more precise noise model, further flight tests will be conducted in October, 2005 to measure the helicopter noise in a wide range of directions using microphones mounted at the tips of cranes, to obtain more precise source and propagation data.

References

- 1) Funabiki, K., Muraoka, K., Iijima, T. and Shiomi, K., "NOCTARN: Trajectory Based CNS/ATM Concept for Small Aircraft," presented at 21st Digital Avionics Systems Conference, Irvine, California, 2002.
- 2) Ochi, A., Aoyama, T., Saito, S., Shima, E., and Yamakawa, E., "BVI Noise Predictions by Moving Overlapped Grid Method", AHS 55th Annual National Forum, Montreal, Canada, 1999.
- 3) Okuno, Y. and Matayoshi, N., "Development of a New Research Helicopter MuPAL-ε" presented at the 57th AHS Annual Forum, Washington DC, 2001.
- 4) Ishii, H., Okuno, Y., and Funabiki, K., "Flight Experiments for Aircraft Noise Measurement Using 'Tunnel-In-the-Sky' Display," AIAA 2002-4880, presented at AIAA Atmospheric Flight Mechanics Conference and Exhibit, Monterey, California, 2002.
- 5) Ishii, H., Gomi, H., and Okuno, Y., "Helicopter Flight Tests for BVI Noise Measurement Using an Onboard External Microphone," AIAA 2005-6119, presented at AIAA Atmospheric Flight Mechanics Conference and Exhibit, San Francisco, California, 2005.
- 6) International Standard Organization, "Acoustics - Attenuation of Sound during Propagation Outdoors - Part 1: Calculation of the Absorption of Sound by the Atmosphere," ISO 9613-1, 1993.

- 7) Society of Automotive Engineering, "Prediction Method for Lateral Attenuation of Airplane Noise during Takeoff and Landing," AIR 1751, 1981.
- 8) Shinohara, N., Makino, K., Tsukioka, H., Yoshioka, H., and Yamada, I., "Evaluation of Excess Ground Attenuation for Noise Prediction Considering Meteorological Conditions," presented at The 33rd International Congress and Exposition on Noise Control Engineering, Prague, Czech Republic, 2004.
- 9) Hargraves, C. R. and Paris, S. W., "Direct trajectory optimization using nonlinear programming and collocation," Journal of Guidance, Control, and Dynamics, Vol. 10, No. 4, 1987.
- 10) Funabiki, K., "Design of Tunnel-in-the-Sky Display and Curved Trajectory," presented at 24th International Congress of the Aeronautical Science, Yokohama, Japan, 2004.